Laser cleaning performance and mechanism in stripping of Polyacrylate resin paint

Haichao Zhao[1] · Yulin Qiao[1] · Xian Du[1] · Sijie Wang[1] · Qing Zhang[2] · Yan Zang[2] · Xiaoting Liu[2]

Abstract

Laser cleaning is a high-efficient, newly emerging and environmentally friendly technology. Removing paint from aircraft skin is an important application of this technology. This paper describes how a high repetition frequency fiber laser of 1064 nm was used to remove the 50-μm-thick polyacrylic resin primer paint layer on an aircraft skin (LY12 aluminum alloy plate). Experiments were conducted to study the cleaning performance by varying process parameters such as scanning speed, pulse frequency, scanning line interval and laser power. This paper found that the quality and efficiency could be improved by selecting the appropriate combination of scanning speed and pulse frequency. The amount of paint stripped by the single pulsed laser increased with an increase in laser power. By analyzing the cleaned surface and the particles collected from the process, we propose three different kinds of possible stripping mechanisms: combustion reaction, thermal stress vibration effect and plasma shock effect.

Keywords Pulsed laser · Polyacrylate resin · Paint stripping · Law · Mechanism

1 Introduction

When large vehicles, such as aircraft and ships, must be overhauled, the previous paint layer on the surface must be removed to check for fatigue cracks and surface defects [1–7]. Traditional paint stripping method includes mechanical paint stripping method, ultrasonic paint stripping method and chemical paint stripping method [8]. Although these paint stripping techniques are well known and widely used, there are many disadvantages. The mechanical paint stripping method easily produces irreversible damage to the substrate, while the process is labor intensive and is very noisy. The area of the paint stripping groove used by ultrasonic paint stripping method limits the sizes and shapes for this technique. The organic cleaning agents used in chemical paint stripping process produce serious environmental contamination and cannot be used when removing paint in specific areas.

Compared with traditional paint stripping methods, laser cleaning technology has the following advantages [9, 10]. There is no direct contact and mechanical damage. Next, there is no environmental pollution and the working environment is clean. In addition, the area to be stripped can be located accurately, the process can be automated, and the procedure can be done over a wide area. Next, real-time monitoring and accurate control of process flow can be achieved. Finally, the process has low operating and maintenance costs. Therefore, research on laser cleaning technology of paint has important practical values and has significant economic advantages. The research should determine the appropriate laser parameters to make the process efficient and safe.

The purpose of laser cleaning is to directly gasify the paint layer by using the laser to destroy the adhesion between paint layer and the surface. Recently, Schweizer et al. used high-power TEA CO_2 laser to remove the paint layer and concluded that the key parameter during the paint stripping process by CO_2 laser was laser power density. In addition, they found that the overlap rate of laser scanning lines had a certain effect on paint stripping efficiency [11]. Chen et al. [12] adopted the fast-axial-flow CO_2 laser with a wavelength of 10.6 μm

✉ Yulin Qiao
  Qiaoyulin1010@sina.com

1 National Engineering Research Center for Mechanical Product Remanufacturing, Army Academy of Armored Forces, Beijing 100072, China

2 Laboratory on Remanufacturing, Army Academy of Armored Forces, Beijing 100072, China

to remove the paint layer on an aluminum plate surface and studied the relationship between the paint layer stripping effect and laser power density, scanning speed and also the overlap amount of scanning paths. The authors pointed out that the laser power density was an important parameter in paint stripping process, and that increasing the power could remove more paint. Shi [13] showed that when the laser power density and scanning overlap rate were in the appropriate range, a better paint stripping result and higher cleaning efficiency could be obtained by increasing laser power, pulse repetition frequency, or increasing spot diameter. Tian [14] analyzed the effect of laser wavelength, pulse duration, laser energy, material properties and other technical parameters on the paint stripping threshold and efficiency during the process. This paper found that the laser pulse duration, laser energy density and the properties of the substrate under the paint had an important impact on paint stripping. Brygo et al. [15] studied the technical characteristics of laser pulse repetition frequency and pulse duration based on the ablation mechanism of paint stripping. Jasim et al. [16] carried out the paint stripping test, which was to remove the white polymer paint on ENAW 5005A aluminum alloy by using Nanosecond Pulsed Fiber Laser. They studied the influence of laser energy, pulse frequency, overlap rate and other process parameters on the ablation size, ablation depth, surface morphology and surface roughness. Barletta et al. [3] adopted a diode array laser to scan the aluminum plate samples with paint layer and studied the effect of laser parameters on the paint stripping efficiency from both experimental and theoretical perspectives. They verified their model by experimental studies. Mateo et al. [17] had found that the paint layer on the brass surface could be removed by a reasonable configuration of laser energy and pulse frequency.

The laser cleaning process of paint on aircraft skin is an important application area of laser cleaning technology [18]. At present, there are relatively few detailed reports of laser cleaning process of paint and a description of the mechanism for this application. In this paper, a high repetition frequency fiber pulsed laser was used to remove the polyacrylic resin paint layer on an aircraft skin (aluminum alloy) surface. We show scanning speed, pulse frequency, scanning line interval and laser power affects the efficiency of removing the paint. In addition, we explored the corresponding action mechanism with the goal of providing a useful reference for this application.

2 Experimental conditions and methods

2.1 Testing equipment and materials

Figure 1 is a schematic diagram of the fiber laser cleaning device, which shows the fiber pulsed laser, a scanning galvanometer and a control card. These items are shown
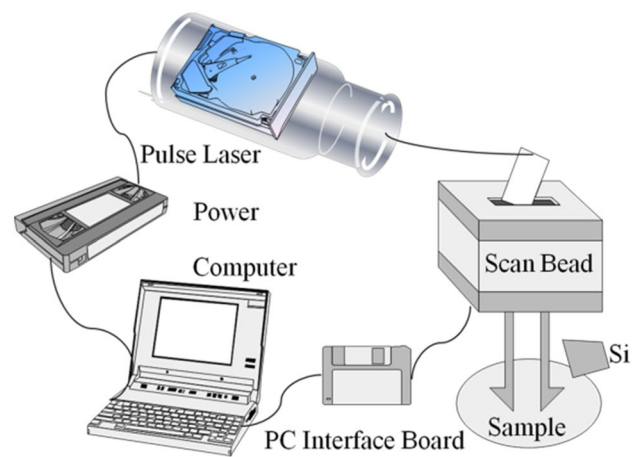
Fig. 1 The schematic diagram of the fiber laser cleaning device

Table 1 The main parameters of the fiber laser

Parameters	Wavelength (nm)	Maximum power (W)	Pulse duration (µs)	Repetition frequency (kHz)	Trigger mode
Parameter values	1064	30	1	20–100	Pulse

in Table 1. The samples had a substrate which was made from LY12 aluminum alloy and had the dimensions of 15 mm × 15 mm × 3 mm. The paint layer on the samples was yellow TB06-9 polyacrylic resin paint layer with the thickness of about 50 µm. A silicon wafer with the size of 2 cm × 2 cm was adopted as a base for collecting particles, which was about 17 mm away from the sample and parallel to the sample surface. It directly faced the ablation hole. During the experimental process, a silicon wafer was placed in an ethanol solution and cleaned ultrasonically for 5 min to remove the surface contaminants.

2.2 Experimental methods

The laser cleaning method for removing paint is shown in Fig. 2. The paint layer on the aluminum alloy plate was 50 mm in thickness. A laser spot focused on the sample and moved systematically by moving the x-axis and y-axis of the vibration mirrors. The laser beam spot of the laser was a series of discontinuous circular spots distributed at a given frequency, and the laser energy had the shape of a Gaussian distribution. The radius [R] and diameter [D] of the laser spot was $D = 78$ µm.

To reduce material waste and energy consumption, we first made a preliminary study. The exploration was conducted by means of single-track processing to reveal the effect of the process variables on the efficiency of
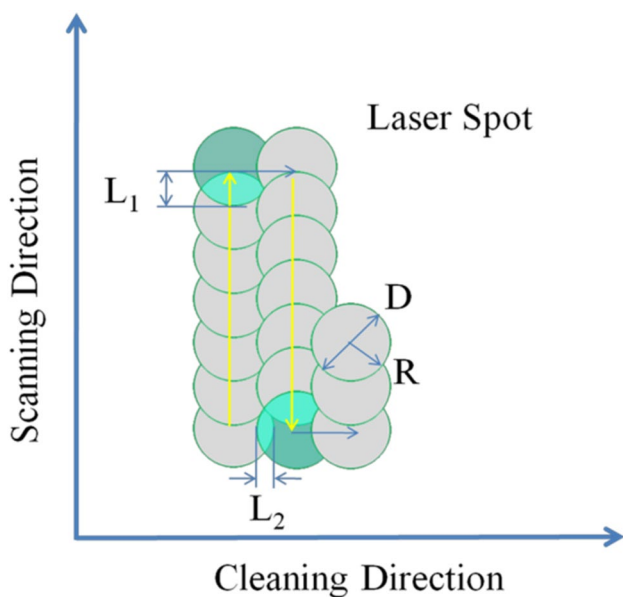
Fig. 2 The cleaning method of paint layer

Fig. 3 The relation graph for the geometric overlap of laser spots

removing the paint. We selected different scanning speeds, pulse frequencies, scanning line intervals and laser power.

The surface morphology feature of the cleaned surface of paint layer on aluminum alloy skin was characterized by the OLYMPUS LEXT-QLS4000 three-dimensional profilometer to determine its surface appearance and surface roughness. At the same time, the depth of the removed paint layer was measured by the OLYMPUS LEXT-QLS4000 three-dimensional profilometer. The surface morphology of the particles collected during the cleaning process was observed using the SIGMA300 field emission scanning electron microscopy.

3 Results and discussion

3.1 Analyzing the effect of scanning speed on pulsed laser cleaning of paint

When removing paint, it is important to lower the energy consumption and reduce the effect of energy overlap between the spots. To parametrize this process, we define the overlap amount between the laser spots as L_1 and the overlap amount between the scanning paths as L_2. Figure 3 shows the two-dimensional geometry of the pulsed laser spots. The overlap rate between spots U_p is mainly determined by the two parameters: pulsed laser frequency f and scan speed v, while the overlap rate between scanning paths U_L is relatively simple, which is the scanning line interval set by the computer control program.
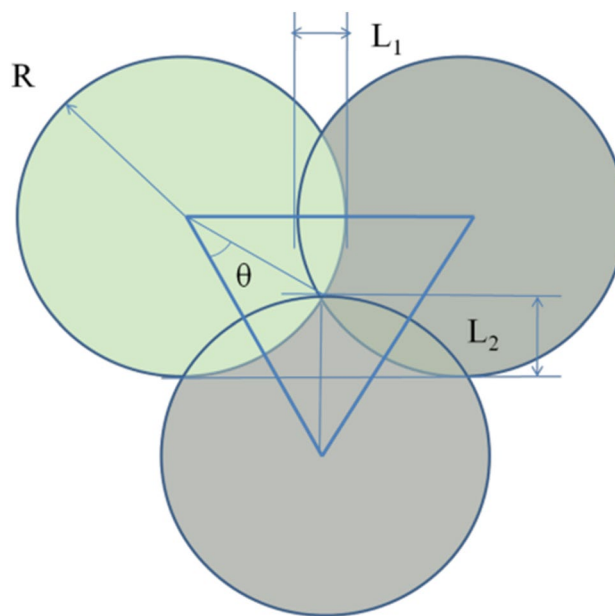
The specific relationship between the spot overlap rate U_p and the scan track overlap rate U_L is shown by Eqs. (1) and (2):

$$U_p = L_1/D \tag{1}$$

$$U_L = L_2/D \tag{2}$$

It can be calculated from Fig. 3 that:

$$L_1 = 2R(1 - \cos\theta) \tag{3}$$

$$L_2 = R(1 - \sin\theta) \tag{4}$$

$$U_p = 1 - \cos\theta \tag{5}$$

$$U_L = 0.5(1 - \sin\theta) \tag{6}$$

It can be seen from the geometrical relationship analysis that, when $\theta = 30°$, the overlap area among the three spots is the smallest, the energy distribution is more uniform, the heat dissipation is better, and the energy utilization rate is the highest. In this case, U_p is 13.4%, and U_L is 25%.

When the pulse frequency of fiber laser was $f = 30$ kHz and the laser scanning speed was v (mm/s), then $L_1 = 2[R - 0.5(v/f)]$ [16, 19] and

$$U_p = 1 - v/(D \cdot f) = 1 - v/2340 \tag{7}$$

During the experimental process, U_p and U_L usually varied in the following ranges: $13.4\% \leq U_p \leq 65\%$

and $0\% \leq U_{\mathrm{L}} \leq 25\%$. Therefore, from Eq. (7) we have the following ranges for velocity and L_2: 819 mm/s $\leq v \leq$ 2026.44 mm/s and 0 mm $\leq L_2 \leq$ 0.0195 mm.

Figure 4 shows the three-dimensional morphology of the surface cleaned by the pulsed laser at different scanning speeds. That figure shows that the pulsed laser can always remove a certain amount of paint at these speeds, and that a "circular" cleaned pit will form. Figure 4a, b shows that when v was 1000 mm/s, there was a significant partly overlap. Figure 4c, d shows when v was 2400 mm/s, the cleaned pits just overlapped. When the scan speed was 2600 mm/s, the cleaned pits completely separated (Fig. 4e, f). After comparing the three-dimensional morphology under different scanning speeds, when cleaning is done under a constant laser power, better cleaning quality can be achieved; when the scanning speed is less and there is a greater overlap rate between the spots, cleaning efficiency will be reduced. When the laser scanning speed is too fast, the overlap rate between the spots is small or even zero. At this time, a single channel scan cannot completely remove the paint layer and also cannot achieve the complete paint stripping on the entire workpiece surface. These observations indicate that the pulsed laser spot needs a certain overlap to completely remove the paint layer. According to Eq. (7), when the scanning speed was 2340 mm/s, the cleaned pit formed by the pulsed laser spot should theoretically be tangent. In practice, the value was 2400 mm/s. This result is because the cleaned pit diameter formed by the single pulsed laser spot was greater than 78 μm (Table 2), so that the cleaned pits formed by the pulsed laser spot still overlapped when the scanning speed was 2340 mm/s.

Due to the use of Gaussian-shaped laser beam, the cleaned pits made with this profile could be obtained from the morphology of the single pit formed after removing a certain part of paint layer [20]. However, according to the specific analysis, both the size and shape of the pits were not exactly the same, and the bottom of the pit was uneven and the pit boundary line was very uneven. There are several reasons for this phenomenon. The laser beam energy was unevenly distributed in the cross section of the beam, the energy density at the beam center was generally larger than that at the edge part, and the spatial stability of the laser beam varied. In addition, there was the Knudsen layer of the laser in the gas–liquid interface of pit [21]. The thickness of Knudsen layer was only a few molecules average free range, and this phenomenon resulted in a discontinuous temperature, density and pressure across this thin layer. The Knudsen layer had a strong shielding effect on heat transfer.

Figure 4 shows that the inside wall of the cleaned pit formed on paint layer surface had both the "slope" shape of smooth transition and the "bluff" shape close to be vertical to paint layer surface. The main reasons for this appearance are:

1. There were small pits on paint layer surface itself, and there was a certain degree of unevenness inside the paint layer, affecting the laser action in different area.
2. As the laser energy had a Gaussian shape, the energy density was highest at the center of circular spot and the energy near the edge of the spot was lower. Thus, the paint layer would be removed only a little in area closer to the edge of spot.

When the energy density was lower than a certain value, the paint layer could not be removed. According to our measurements, the diameter of a pit formed by the laser was about 85–100 μm, and the maximum depth of the removed paint layer was 20–22.5 μm. The diameter of the cleaned pit was greater than the theoretical diameter of laser spot 78 μm, which was mainly caused because the paint layer near the spot also reached the stripping condition which expanded the area of the pulsed laser spot.

Figure 5 shows the cleaning trace for five different single-track scans. Table 2 shows the parameters of these scans. Figure 5 shows that for the first three scans, the color of the paint layer surface in the scanning area became darker, and part of the paint layer in the scanning area was removed, while the aluminum alloy substrate could not be seen. Combined with the data in Table 2, it can be seen that the diameter, depth and volume of the pits on the cleaned surface were gradually increased versus trial number. The diameter of these pits did not change significantly, but the depth and volume of the pits did change significantly. The amount of removed paint gradually increased with each scan. At Scan 4, the paint began to partially separate from the substrate. Most of the paint layer was removed, and part of the substrate had been exposed with the visible metallic luster was visible.

The stripping amount of paint layer could be controlled by adjusting the overlap rate between laser beams, realizing a good cleaning. Therefore, according to the results of single-track scans, it can be found that the paint layer could be completely removed when the laser scanned for 3 to 4 times. Figure 6 shows a schematic diagram of overlap of laser spots. U_{p} should be in the range, $66.6\% \leq U_{\mathrm{p}} \leq 75\%$, to completely remove the paint layer. It can be calculated from Eq. (7) that 585 mm/s $\leq v \leq$ 780 mm/s.

3.2 Analyzing the effect of pulse frequency on laser cleaning of paint

Figure 7 shows the three-dimensional morphology of the cleaned pits on the cleaned surface as a function of different laser pulse frequencies. Combined with the data in Table 3, it can be seen that with the increase in pulse frequency, the overlap rate of pulsed laser spot gradually increased, the single pulse energy gradually decreased, and the paint
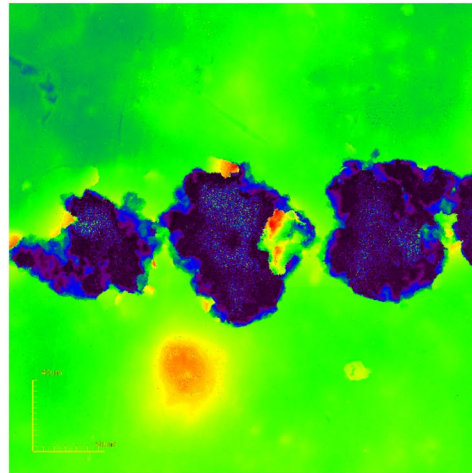
Fig. 4 3D morphology of pits on paint layer surface at different scanning speeds (power: 16.5 W; repetition frequency $f = 30$ kHz)
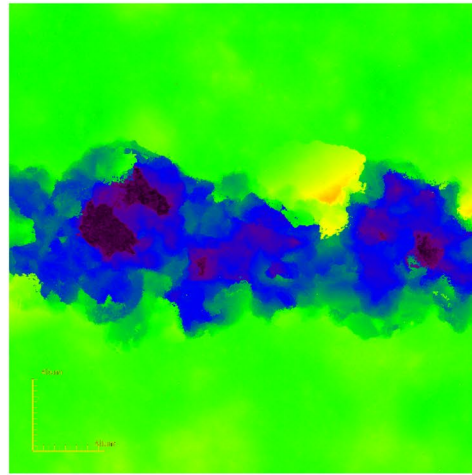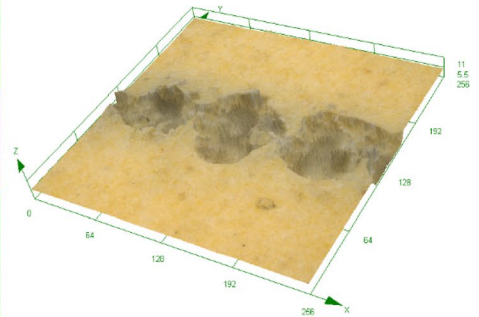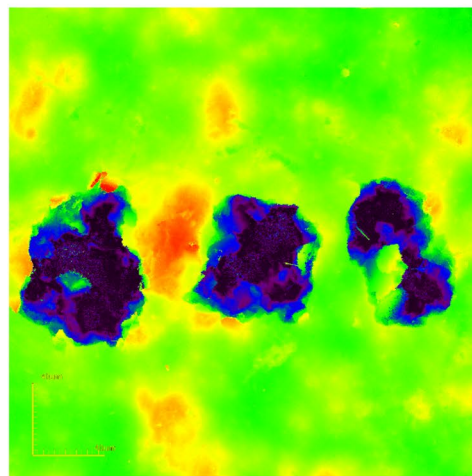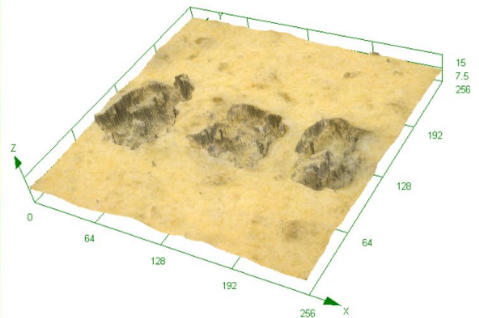

(a) 1000 mm/s.
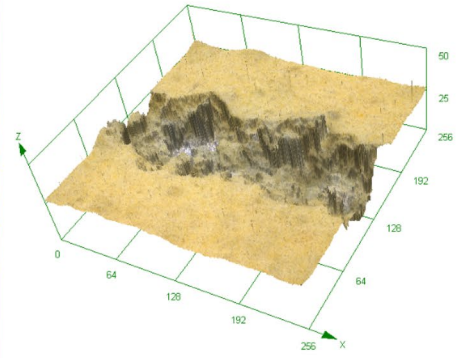
(b) 1000 mm/s.

(c) 2400 mm/s.

(d) 2400 mm/s.

(e) 2600 mm/s.

(f) 2600 mm/s.

Table 2 The parameters of cleaned pits obtained after different times of single-track scanning

Process parameters	Power: 16.5 W, Repetition frequency $f=30$ kHz, scanning speed: 2400 mm/s				
Scan number	1	2	3	4	5
Average spot diameter (μm)	98.785	100.051	110.97	113.513	115.257
Average cleaning depth (μm)	21.321	26.578	34.015	48.437	49.368
Stripping volume of paint layer ($\times 10^4$ μm^3)	6.40	8.42	15.70	18.96	20.52

Fig. 5 The cleaning marks after different times of single-track scanning (power: 16.5 W; scanning speed: 2400 mm/s; repetition frequency $f=30$ kHz)
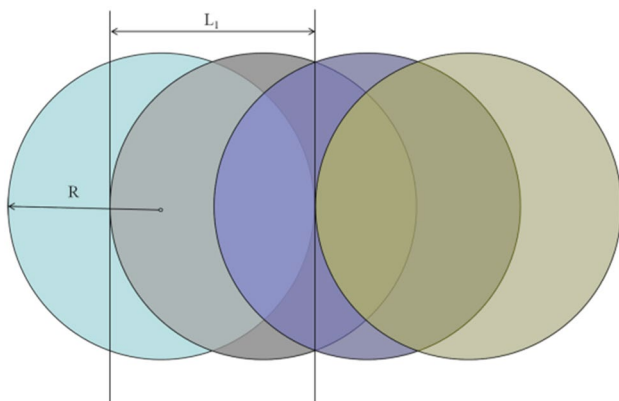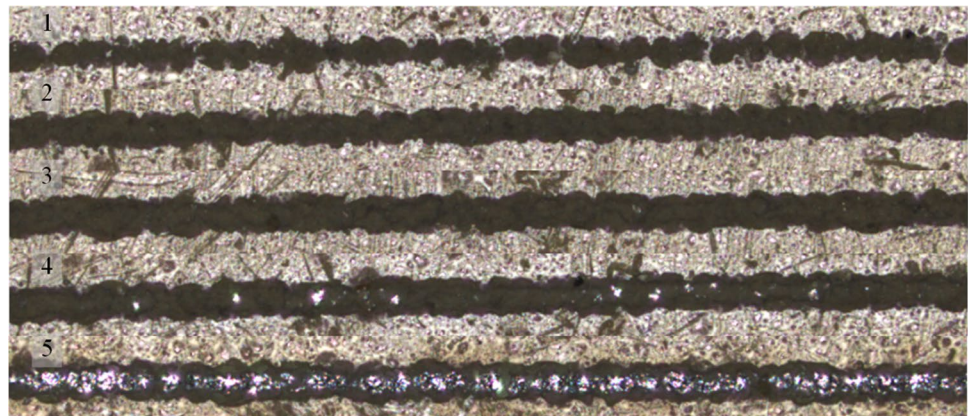

Fig. 6 A schematic diagram of overlap of laser spots

stripping amount of the single pulse increased first and then decreased. The data show that the amount of paint removed was not only related to the spot overlap rate but also affected by the pulse energy. According to our analysis, when the pulse frequency was too low, the energy of a single pulse was too high, and a plasma shielding effect would be generated near the paint layer surface. The heat energy produced by the light could be absorbed by the plasma, while the paint layer absorbed less heat, and therefore, the stripping amount of paint layer became less. Figure 7e shows when the pulse frequency was too high, even if the overlap rate of laser spot was very high, the energy of a single pulse was very small,

and therefore, the paint layer absorbed very low energy, which could not remove most of the paint layer.

To better explain the impact of pulse frequency on the stripping effect of paint layer, the concept of stripping rate was defined. The stripping rate of paint layer during laser irradiation process is defined as follows [22]:

$$\eta = \sqrt{\frac{E}{\rho}} \frac{\alpha \varepsilon}{\rho ch} \tag{8}$$

where ε is a single pulse energy of laser, h is the thickness of paint layer, E is the elastic module of paint layer, ρ is the density of paint layer, α is the expansion coefficient of paint layer, c is the specific thermal capacity of paint layer. Regardless of the plasma shielding effect, it can be shown from Eq. (8) that because the energy ε of a single laser pulse will be reduced with the increase in pulse frequency when the laser power is constant, the stripping rate of paint layer will also be reduced.

3.3 Analyzing the effect of scanning line interval on laser cleaning of paint

Figure 8 shows the three-dimensional morphology of the cleaned surface by the pulsed laser with different scanning line intervals. The figure shows that as scanning line interval is increased, the residual amount of paint layer on the cleaned surface increased, and the cleaning effect decreased.
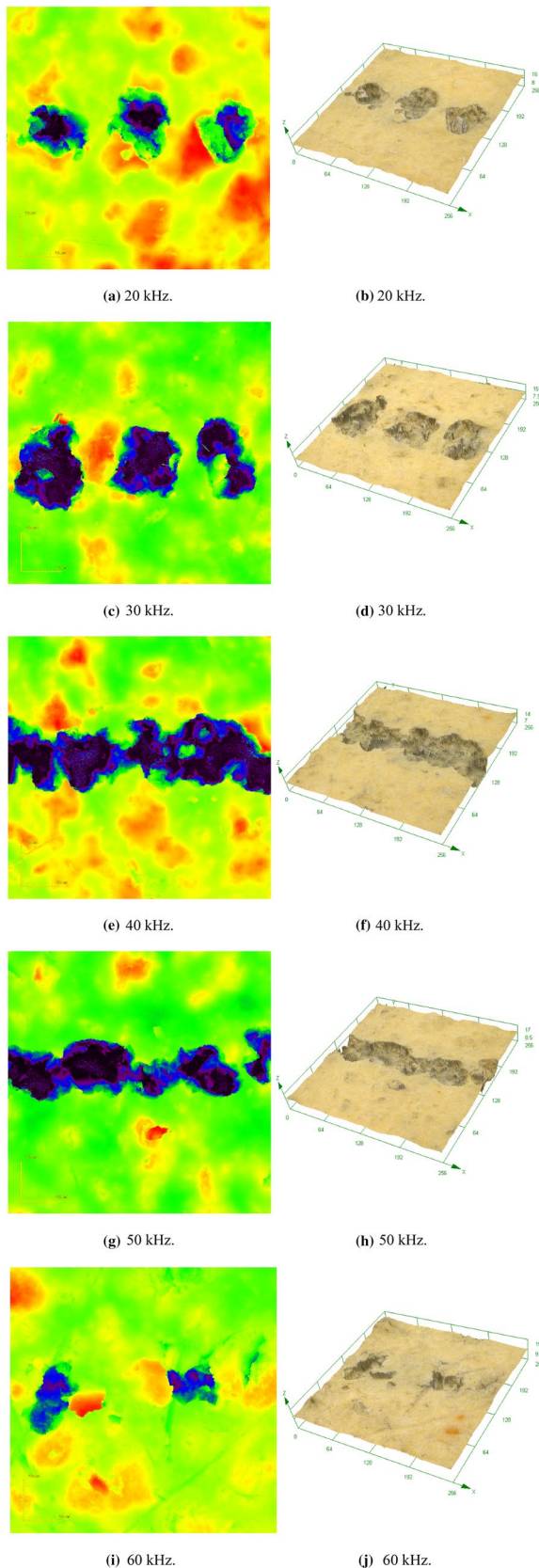
(a) 20 kHz.   **(b)** 20 kHz.

(c) 30 kHz.   **(d)** 30 kHz.

(e) 40 kHz.   **(f)** 40 kHz.

(g) 50 kHz.   **(h)** 50 kHz.

(i) 60 kHz.   **(j)** 60 kHz.

Fig. 7 The three-dimensional morphology of the cleaned pits on paint layer surface at different pulse frequencies (16.5 W, 2600 mm/s)

When the scanning line interval was 0.01 mm, as shown in Fig. 8a, a large area of aluminum alloy substrate had been exposed on the cleaned surface. This figure shows that when the scanning line interval was small, the overlap rate of pulsed laser spot was large; the accumulation of energy on paint layer surface was too high. This process resulted in a large amount of paint was removed. When the scanning line interval was 0.05 mm and 0.07 mm, obvious laser scanning paths could be seen on the cleaned surface, and the complete paint layer still existed in the edge area of the scans. Figure 8e, g indicates that when the scanning line interval was too large, the paint layer absorbed insufficient energy and the stripping amount of paint layer was reduced. When the scanning line interval was 0.03 mm, the pulsed laser spots were evenly distributed on paint layer surface and could completely cover the paint layer surface. In addition, the absorption energy in various regions of the paint layer was more uniform, and the aluminum alloy substrate and complete paint layer could not be observed on the cleaned surface (Fig. 8c, d).

As can be seen from Fig. 8g, h, there were significant differences in morphology along the laser scanning direction and cleaning direction. These observations can be explained because there was heat transfer and an instantaneous temperature rise in the area covered by laser spot and its adjacent areas. Because of the very short interval between the two adjacent laser spots along the laser scanning direction, the above areas had not cooled when the next laser spot acted on the paint layer. The adjacent two laser spots resulted in the energy superposition in the overlap area and its adjacent areas, and the heating area of the paint layer was increased, which could lead to removal of more paint. While, there was no energy superposition effect or the superposition effect was weak due to the long-time interval of two adjacent laser spots along the cleaning direction, there was a difference in the morphology of cleaned surface.

Table 4 shows the surface roughness after laser cleaning with different scanning line intervals. It can be seen that when the scanning line interval was 0.03 mm, the roughness of cleaned surface was the largest with Ra = 3.149 µm. Combined with Fig. 8, the analysis showed that the energy of the pulsed laser had a Gaussian shape with the highest of the energy density at the center of the circular laser spot and the lower of the energy density far from the center of the laser spot. During the cleaning process, the high energy density area (abbreviated as H area) and low energy density area (abbreviated as L area) keeping a certain configuration rule were formed on the cleaned surface. The cleaning depth in H area was large, while the cleaning depth in L area was small. When the scanning line interval was below 0.03 mm, the cleaned surface was entirely covered by the formed H area and L area, and there was no laser spot unaffected area. Therefore, it resulted in an increase difference in the depth

Table 3 The laser process parameters at different pulse frequencies

Pulse frequency (kHz)	20	30	40	50	60
Overlap rate (%)	− 66.67%	− 11.11%	16.67%	33.37%	44.45%
Average power density (W/cm^2)	3.45×10^5				
Single pulse energy (mJ)	0.82	0.55	0.41	0.33	0.27
Energy density (J/cm^2)	17.26	11.51	8.63	6.91	5.76

between H area and L area, and ultimately increased the surface roughness.

3.4 Analyzing the effect of laser power on laser cleaning of paint

Table 5 shows the parameters of cleaned pits on the cleaned surface under the conditions of different pulsed laser power values. It can be seen that with the increase in laser power, the depth of cleaned pits gradually increased and the diameter and volume of the pits increased. The spot diameter D was 61.804 μm that did not reach the theoretical spot diameter of 78 μm when the laser power was 10.5 W. When the laser power was greater than 13.5 W, the spot diameter D was greater than the theoretical spot diameter of 78 μm.

Since the area of pulsed laser spot was very small relative to the paint layer surface, the cleaning process could be regarded as a point heat source heating the semi-infinite object. The temperature model [23, 24] is:

$$\Delta T = \frac{P_{\text{avg}} \sqrt{\alpha \tau}}{0.885K} \tag{9}$$

where P_{avg} is the laser power of laser, α is the thermal diffusivity of material, τ is the laser action time, K is the thermal conductivity coefficient of material. It can be seen from Eq. (9) that the temperature rise of the paint layer surface is linearly related to the laser power. As the power increases, the surface temperature rises. In other words, when the paint layer absorbs much pulse energy, increasing the depth of the spot, the stripping volume of paint layer will increase. However, above laser power values of 16.5 W, the increase in the diameter of the pits formed on the paint layer surface abruptly flattens off and the diameter of the pits tends toward an asymptotic value. This was the result of the presence of strong absorption and scattering of incident laser by the laser generated vapor plume and plasma. When the laser power was 19.5 W, the diameter of the pit was just $D = 86.12$ μm, indicating that the part of laser pulse energy that actually reached the paint surface was reduced, and therefore, the plasma impact was reduced to some extent. At a laser power of 22.5 W, the laser was not completely shielded, and the laser could still pass through the laser plasma layer to reach the surface of the paint due to the increase in power, thus resulting in the increases of the energy absorbed by the

paint, which made the diameter of the pits increase again, $D = 99.671$ μm, indicating the saturation of the diameter of pits.

3.5 Action mechanism analysis

Through our experimental observations and analysis, the action mechanism of the laser to remove the polyacrylic resin paint layer on the aluminum alloy surface may not be explained by a single mechanism. The action mechanism includes the following three kinds: the combustion mechanism, the thermal stress vibration effect and the plasma impact effect.

Figure 9 shows the three-dimensional morphology of the pit on the cleaned surface by the pulsed laser with power of 10.5 W. As can be seen from Fig. 9a, after the action of pulsed laser, the action area of laser spot could be obviously divided into three regions:

1. *The pulsed laser spot irradiated area*, namely the melting area. The focused laser beam center had an ultra-high peak power, and the heat was concentrated. The high energy made the region melt, splash and other processes, forming a damage pit with clear edge owing to melting.
2. *The pulsed laser spot irradiated edge area*, namely thermal influence area. The thermal conduction in the paint layer made the temperature in the outside area of the damaged pit rise, but the area only showed a slight color change due to the low energy.
3. *No laser influence area*. There was no significant change in the paint layer outside the thermal influence area. When paint layer surface absorbed the laser, it quickly absorbed the energy, and converted the laser energy.

Because the thermal conductivity of the paint layer was very low, the laser energy accumulated on paint layer surface, resulting in the rapid increase in surface temperature to reach and exceed the melting point, boiling point and combustion point of the paint. Therefore, the processes such as instant gasification and volatilization of the paint layer and heat combustion occurred. The spherical end morphology, which was formed by the re-solidifying of the melted paint layer, can be seen in Fig. 9b, d. At the same time, there could be a fast thermal explosion due to combustion mechanism.

Fig. 8 3D surface morphology of the cleaned surface at different scanning line intervals (2400 mm/s, 30 kHz, 16.5 W)
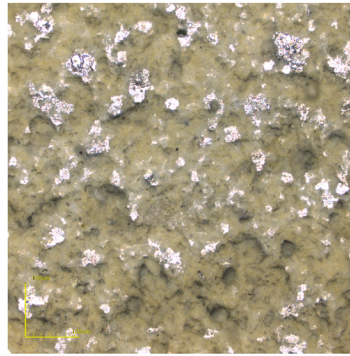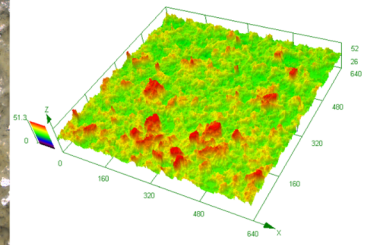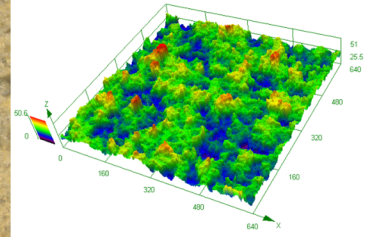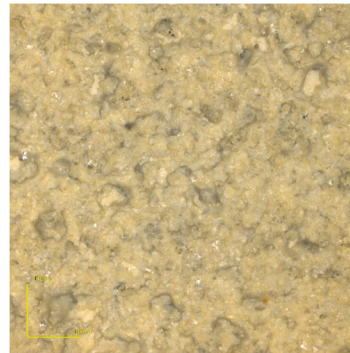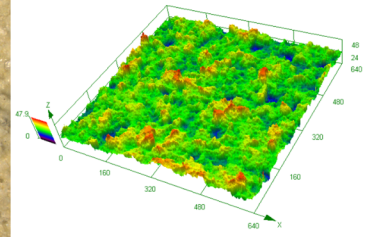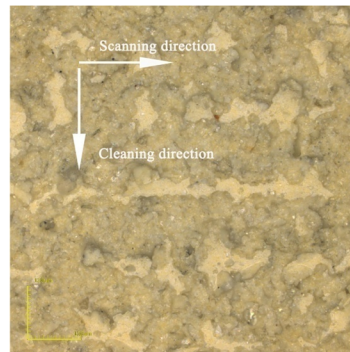

(a) 0.01mm.   (b) 0.01mm.
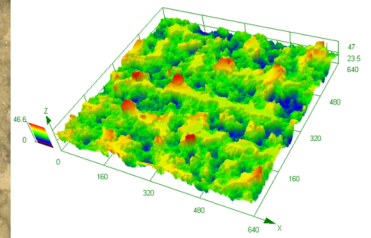
(c) 0.03mm.   (d) 0.03mm.

(e) 0.05mm.   (f) 0.05mm.

(g) 0.07mm.   (h) 0.07mm.

Table 4 The surface roughness after laser cleaning with different scanning line intervals

Scanning line interval (mm)	0.01	0.03	0.05	0.07
Surface roughness Ra (µm)	2.406	3.149	2.736	2.942

As shown in Fig. 9b, it can be seen that there is a large number of small-sized impact marks in the cleaned pit, thus confirming a strong thermal explosion shock.

Since the distribution of pulsed laser spot energy was Gaussian, during the interaction with the paint layer, the energy in the central position was higher and instantaneously transmitted, but a temperature gradient was formed along the horizontal and vertical directions inside the paint layer. The thermal stress transmitted from the heated area to the surroundings and then extended to the entire material [25]. Therefore, the integrity of the polyacrylic polymer molecular chain was destroyed, the cohesive force of the paint layer of high polymer was destroyed, and the inside of the paint layer broke and expanded outwards and splashed, causing a bulge at the edge of pit, as shown in Fig. 9b.

After loading the pulse laser, a large amount of gas and particles accumulated on the surface of the paint layer due to melting, vaporization and even decomposition of the paint. Therefore, a large number of nano- and micro-scale aerosols were generated above the surface of the paint layer. Thus, the breakdown threshold of aerosols would be decreased by about 2 to 3 orders of magnitude, which made the high temperature and pressure plasma shock wave easier to form [26, 27]. Yuan and Zhou [28] proposed empirical criteria for laser plasma, which can be given by:

$$\left[P/(\mathrm{W \cdot cm^{-2}})\right]^{\frac{2}{3}} \left[t/s\right]^{0.5} \left[\lambda/\mu m\right]^{0.36} > (0.95 \sim 1.5) \times 10^2 \tag{10}$$

If we assume that the selected P is increased by two orders of magnitude. It is interesting to note that all the selected P is in accordance with Eq. (10). As a result, aerosols above the paint surface had been ionized to generate laser plasma with high temperature and pressure. During the cleaning process, a popping sound was heard and a flash was seen with the laser loading to the paint.

Phipps et al. [29] suggested an empirical Equation for the impulse coupling coefficient of laser plasma:

$$c_m = b_0\left(I_a\lambda\sqrt{\tau}\right)^h \tag{11}$$

and pressure of laser plasma for removal of paint will be:

Table 5 The parameters of cleaned pits on the cleaned surface under the conditions of different pulsed laser powers (2400 mm/s, 30 kHz)

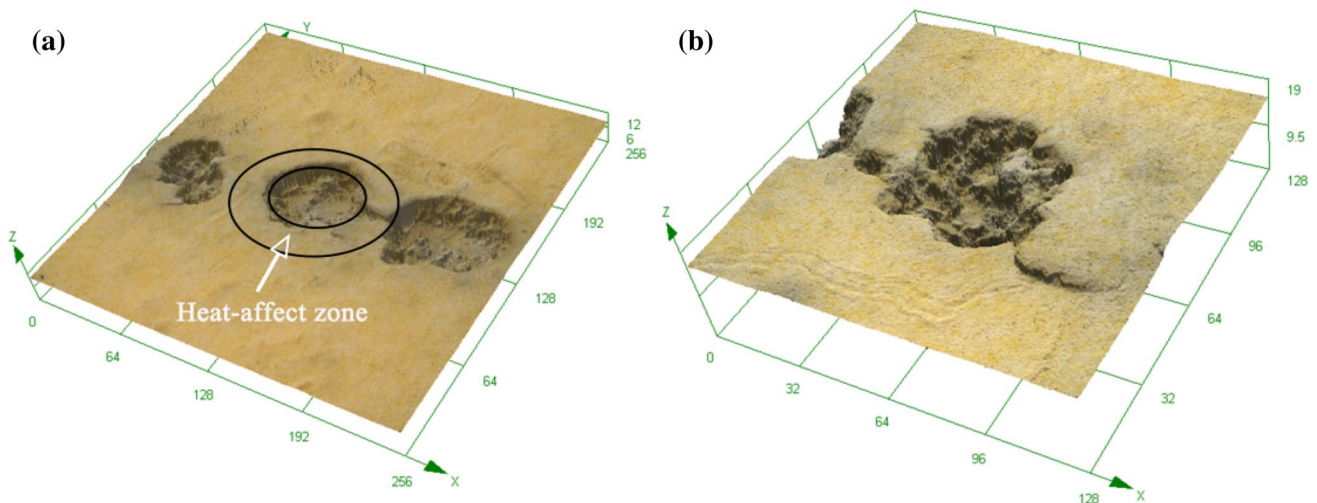| Power (W)	10.5	13.5	16.5	19.5	22.5
Average power density ($\times 10^5$ W/cm^2)	2.20	2.83	3.45	4.08	4.71
Energy density (J/cm^2)	7.32	9.42	11.51	13.60	15.70
Average cleaning depth (µm)	12.512	18.169	21.321	22.389	24.383
Average diameter of pit (µm)	61.804	83.840	98.785	86.120	99.671
Stripping volume of paint layer ($\times 10^4$ µm^3)	1.25	3.75	6.40	5.31	6.87

Fig. 9 The 3D morphology of the pit on the cleaned surface by the pulsed laser with power of 10.5 W (2400 mm/s, 30 kHz)

$$P = b_0 \left(\lambda \sqrt{\tau} \right)^h I_a^{h+1} \qquad (12)$$

where I_a, τ, λ are the absorbed power density, pulse duration and wavelength of incident laser, respectively. b_0 and h are determined by the material of sample; here, we take as $b_0 = 0.5$, $h = -0.3 \pm 0.03$ for carbon–hydrogen materials.

Within the range of selected power density, the minimum pressure of the laser plasma shock on the surface of the paint calculated according to Eq. (12) is 1.53 MPa. The tensile strength of the paint at room temperature is only 1.4–4 MPa [30], which would become lower under the action of combustion, thermal explosion and thermal stress. Therefore, the paint would be removed under the shock of laser plasma.

Figure 10 shows a three-dimensional morphology of the cleaned surface by the pulsed laser with the laser power of 16.5 W and also the morphology of the pit formed on the cleaned surface. Obvious traces of plasma shock, which is the "circular" shape on the cleaned surface, can be observed in Fig. 10a–c. Figure 10d clearly shows the remaining fragments of the paint layer in the pit, which were formed because of impact. In addition, the plasma formation process was accompanied with the absorption of laser energy by paint layer. When the plasma expanded to a certain extent, a certain thickness of isolation layer would be formed between the laser and the paint layer, greatly reducing the laser energy reaching the paint surface. As shown in Table 5 that the diameter of the pit was slightly reduced with the laser power values of 19.5 W.
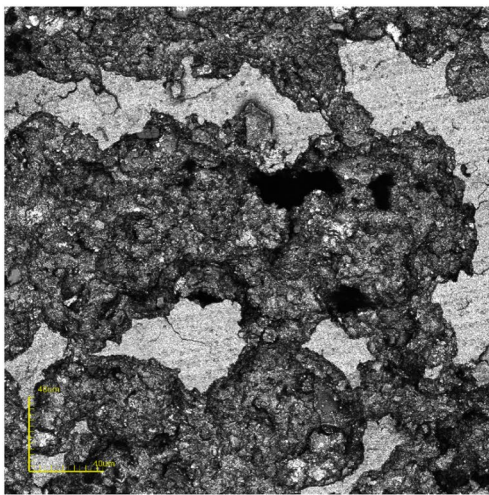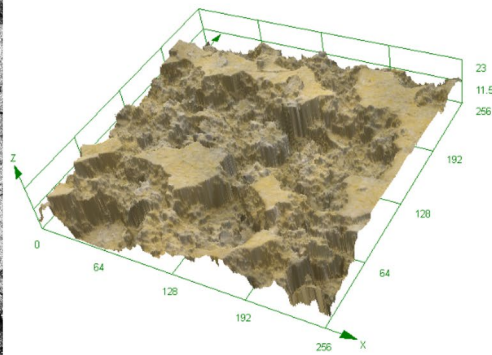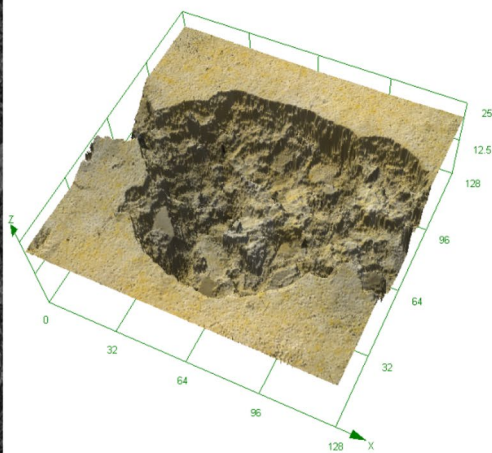

(a) 16.5W, 2400mm/s, 30kHz, 0.03mm.   **(b)** 16.5W, 2400mm/s, 30kHz, 0.03mm..
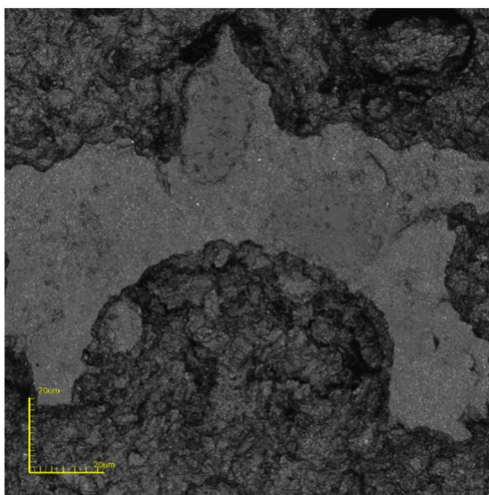
(c) 16.5W, 2400mm/s, 30kHz, 0.03mm.   **(d)** 16.5W, 30kHz, the pit formed by single track scan.

Fig. 10 The 3D morphology of the cleaned surface

Figure 11 displays the SEM images of the particles collected during the paint stripping process when the scanning line interval was 0.03 mm. It can be seen that the collected particles were irregular in shape, and the particles had a clear crack structure (as shown by the circled areas 2, 3 and 4). Meanwhile, it can be seen the complete surface structure of the paint layer (as shown by the circled area 1), indicating that these particles are formed under mechanical action including both the thermal stress and plasma impact force.

During the laser-paint interaction, the rapid expansion of laser plasma can produce strong shock with high pressure on the surface of the paint. According to Eq. (12), the force distribution of the shock is closely related to the radiation intensity of incident laser. For the laser pulse with Gaussian distribution in space and time, the maximum pressure of shock is in the center of laser beam and decreases along the radial direction. Under the impact of shock, the paint in the center of laser beam would break vertically; meanwhile, tension is generated within the paint which made cracks occur within the paint around the center of laser beam. However, there is a competitive relationship between the cracks within paint under the repeated impact of multiple pulses and continues effect of thermal vibration. Comparative analysis shows that some cracks would expand, extend and directly
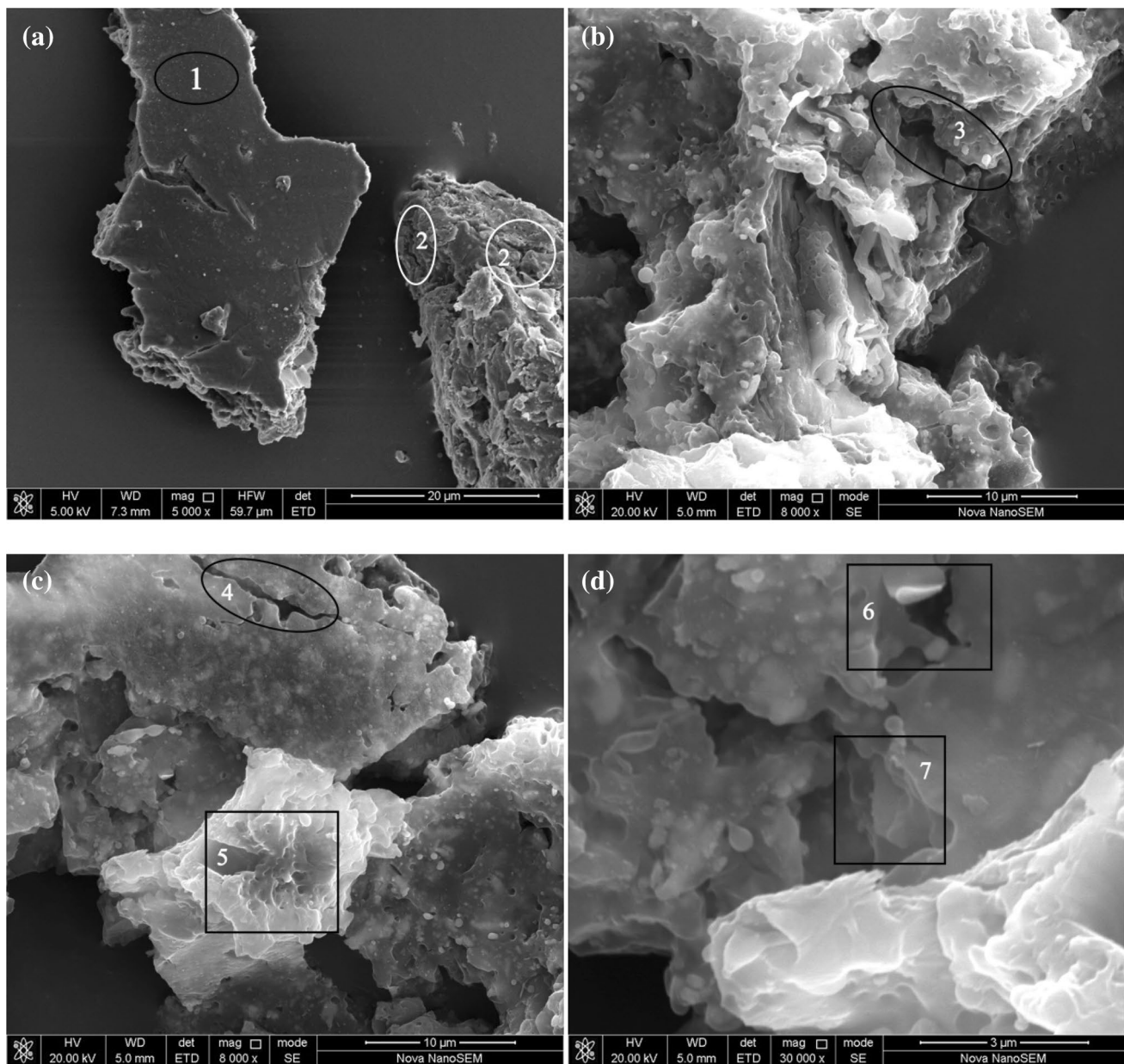

Fig. 11 The SEM images of the particles collected during the paint stripping process when the scanning line interval was 0.03 mm
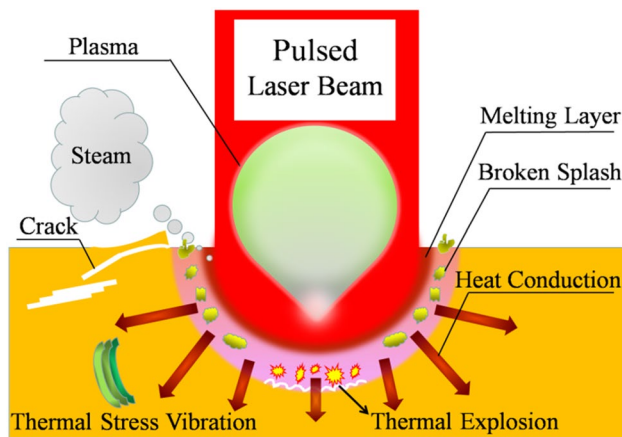
Fig. 12 The schematic diagram for the pulsed laser cleaning mechanism

penetrate with causing damage and fracture of the paint, while some cracks failed to extend and grow, where the paint would not be broken. As for the different results of competitive relationship, the fault-like structure (rectangular areas 5, 7) was formed on the fractured section of paint due to the plasma impact and accompanying thermal stress, while the warped paint layer (rectangular area 6) was also produced [31].

The above analysis shows that when using pulsed laser to clears the polyacrylic resin paint layer on the aluminum alloy surface, there may be the coupling mechanism, which is composed of the simultaneous combustion, thermal stress vibration effect, plasma shock and other processes. The laser cleaning process parameters will affect the action degree of each mechanism. The schematic diagram of pulsed laser cleaning mechanism of paint is shown in Fig. 12.

4 Conclusions

A pulsed laser was used to remove the paint layer on the surface of an aluminum alloy. The influence law of process parameters on paint layer stripping was studied, and the paint layer stripping mechanism was analyzed by characterizing the morphology of the cleaned surface and the particles collected during the cleaning process. The following conclusions can be made:

1. The scanning speed and pulse frequency controlled the energy absorbed by paint layer through adjusting the single pulse energy and the overlap rate of laser spots. The quality and efficiency of laser cleaning of paint could be improved by selecting the appropriate scanning speed and pulse frequency.

2. The scanning line interval affected the change of the cleaned surface roughness, and its effect on the microscopic morphology of cleaned surface was different compared with the overlap of pulsed laser spots. Having a too small scanning line interval made the scan track overlap rate too high, causing damage to the substrate. While, too large scanning line interval could not make the pulsed laser spots completely cover the paint layer surface, it reduced the paint stripping quality.

3. The greater the average laser power, the greater the cleaned depth. The diameter and volume of the pit on the cleaned surface increased with the increase in laser power.

4. The stripping process of paint layer on aluminum alloy surface contained three main mechanisms: one was the combustion mechanism, which meant the paint layer absorbed heat to carry out melting, evaporation and gasification; the second was thermal stress vibration mechanism, which meant the temperature gradient and rapid heating and rapid cooling inside the paint layer, producing a non-uniform heating of painting layer; the third was plasma shock effect, which was caused by the formation of plasma near the surface of paint layer.

Compliance with ethical standards

Conflict of interest The authors declare that they have no conflict of interest.

References

1. John S. Foley, Philip A. Barone, Met. Finish. **90**, 48 (1992)
2. J.H. Scholten, J.M. Teule, V. Zafiropulos, R.M.A. Heeren, J. Cult. Herit. **1**, S215 (2000)
3. M. Barletta, A. Gisario, V. Tagliaferri, J. Mater. Process. Technol. **173**, 232 (2006)
4. V. Tornari, V. Zafiropulos, A. Bonarou, N.A. Vainos, C. Fotakis, Opt. Lasers Eng. **34**, 309 (2000)
5. S. Siano, J. Agrest, I. Cacciari, D. Ciofine, M. Mascalchi, I. Ostcioli, A.A. Mencaglia, Appl. Phys. A **106**, 419 (2012)
6. C. Zhang, C. Yao, C. Wang, Optik **127**, 3750 (2016)
7. G. Yang, H.H. Liu, J.P. Zhou, L.Y. Qin, W. Wang, Y.H. Ren, Infrared Laser Eng. **46**, 0206004 (2017)
8. L. Li, D.Q. Zu, China Shiprep. **28**, 13 (2015)
9. T. Kim, J.M. Lee, S.H. Cho, T.H. Kim, Opt. Laser Eng. **43**, 1010 (2005)
10. G.X. Chen, T.J. Kwee, K.P. Tan, Y.S. Choo, M.H. Hong, Appl. Phys. A **101**, 249 (2010)
11. G. Schweizer, L. Werner, SPIE **2502**, 57 (1995)
12. J.F. Chen, Y.K. Zhang, R.J. Xu, Y.Y. Gu, X.Q. Zhang, Laser Technol. **32**, 64 (2008)

13. S.D. Shi, P. Du, W. Li, F. Song, C. Wang, N.J. Cheng, Chin. J. Laser **39**, 0903001 (2012)
14. B. Tian, W.F. Zou, Z. He, S.J. Liu, F. Song, Clean World **23**, 1 (2007)
15. F. Brygo, C. Dutouquet, F. Le Guern, R. Oltra, A. Semerok, J.M. Weulersse, Appl. Surf. Sci. **252**, 2131 (2006)
16. H.A. Jasim, A.G. Demir, B. Previtali, Z.A. Taha, Opt. Laser Technol. **93**, 60 (2017)
17. M.P. Mateo, T. Ctvrtnickova, E. Fernandez, J.A. Ramos, A. Yanez, G. Nicolas, Appl. Surf. Sci. **255**, 5579 (2009)
18. D.J. Wu, Y. Xu, X.Y. Wang, R.K. Kang, Y. Sima, L.Z. Hu, Opt. Precis. Eng. **14**, 764 (2006)
19. H. Zhang, W.W. Liu, Y.Z. Dong, J.C. Cheng, H.C. Zhang, Laser Optoelectron. Prog. **50**, 12140 (2013)
20. Y.F. Lu, T.E. Loh, H.G. Soh, T.S. Low, Appl. Surf. Sci. **90**, 217 (1995)
21. Y.L. Yao, H.Q. Chen, W.W. Zhang, Int. J. Adv. Manuf. Technol. **26**, 598 (2005)
22. Y. Zhang, Ome Inf. **25**, 22 (2008)
23. F. Song, W.F. Zou, B. Tian, S.J. Liu, K.Z. Niu, X.P. Li, J.G. Tian, Chin. J. Laser **34**, 1577 (2007)
24. Y. Luo, X. Wang, H.F. Zhao, F.T. Tian, Appl. Laser **37**, 544 (2017)
25. J.M. Lee, K.G. Watkins, J. Appl. Phys. **89**, 6496 (2001)
26. P. Dewalle, J. Vendel, J.M. Weulersse, P. Hervé, G. Decobert, Aerosol Sci. Technol. **10**, 902 (2010)
27. D.C. Smith, Appl. Phys. **6**, 2217 (1977)
28. G. Yuan, G.Q. Zhou, Chin. J. High Press. Phys. **2**, 182 (1988)
29. C.R. Phipps Jr., T.P. Turner, R.F. Harrison, G.W. York, W.Z. Osborne, G.K. Anderson, X.F. Corlis, L.C. Haynes, H.S. Steele, K.C. Spicochi, Appl. Phys. **3**, 1083 (1988)
30. J. Yang, J.H. Han, T. Duan, N.C. Sun, C. Guo, G.Y. Feng, Q.X. Liu, Laser Technol. **6**, 718 (2013)
31. X.K. Li, Q.H. Zhang, X.Z. Zhou, D.Q. Zhu, Q.X. Liu, Optik **156**, 841 (2018)